Hindawi
Advances in Civil Engineering
Volume 2022, Article ID 5229911, 20 pages
https://doi.org/10.1155/2022/5229911

Review Article

Review of InfraRed Thermography and Ground-Penetrating Radar Applications for Building Assessment

Iván Garrido,[1] **Mercedes Solla**,[1] **Susana Lagüela**,[2] **and Mezgeen Rasol**[3]

[1]*CINTECX, Universidade de Vigo, GeoTECH Research Group, Campus Universitario de Vigo, As Lagoas, Marcosende, Vigo 36310, Spain*
[2]*TIDOP Research Group, EPS Ávila, Universidad de Salamanca, Calle Hornos Caleros 50, Avila 05003, Spain*
[3]*Université Gustave Eiffel, MAST/EMGCU, 5 Boulevard Descartes, 77454 Marne-la-Vallée Cedex 2, Paris, France*

Correspondence should be addressed to Iván Garrido; ivgarrido@uvigo.es

Received 7 May 2022; Revised 26 July 2022; Accepted 9 August 2022; Published 5 September 2022

Academic Editor: Alessandro Rasulo

The first appearance of concern for the good condition of a building dates back to ancient times. In recent years, with the emergence of new inspection technologies and the growing concern about climate change and people's health, the concern about the integrity of building structures has been extended to their analysis as insulating envelopes. In addition, the growing network of historic buildings gives this sector special attention. Therefore, this study presents a comprehensive review of the application of two of the most common and most successful Non-Destructive Techniques (NDTs) when inspecting a building: InfraRed Thermography (IRT) and Ground-Penetrating Radar (GPR). To the best knowledge of the authors, it is the first time that a joint compilation of the state-of-the-art of both IRT and GPR for building evaluation is performed in the same work, with special emphasis on applications that integrate both technologies. The authors briefly explain the performance of each NDT, along with the individual and collective advantages of their uses in the building sector. Subsequently, an in-depth analysis of the most relevant references is described, according to the building materials to be studied and the purpose to be achieved: structural safety, energy efficiency and well-being, and heritage preservation. Then, three different case studies are presented with the aim of illustrating the potential of the combined use of IRT and GPR in the evaluation of buildings for the purposes defined. Last, the final remarks and future lines are described on the application of these two interesting inspection technologies in the preservation and conservation of the building sector.

1. Introduction

Building assessment is becoming more and more common within the construction sector because buildings are physical assets that provide habitat and comfort for people [1]. As an added value, heritage buildings evidence the evolution of humanity and provide cultural, spiritual, and aesthetic satisfaction to the people, as well as economic benefits through tourism [2]. Proof of this importance is more than 1,100 standards published by the International Organization for Standardization (ISO) that help codify international best practices and technical requirements to ensure that buildings are safe and fit for use [3]. Heritage buildings have a distinct category within the ISO standards due to their particular construction and longevity of materials [4]. In addition, all the ISO standards are periodically updated, regardless of their nature, to take into account climatic, demographic, and social changes.

ISO has more than 100 standards [3] related to the raw materials used in construction, such as concrete, cement, timber, and glass. The different properties (structural, mechanical, electrical, thermal, and others) of the building materials mean that the basis of the inspection is different depending on the structural component to be analyzed. Moreover, the boundary conditions of each case study should be taken into account due to the different meteorological and interior control conditions of each building. In the absence of good maintenance conditions in a building,

different surface and subsurface anomalies can appear, causing impairment:

(i) To the structural health of the building. The irreversible collapse of the building materials can be provoked, endangering the integrity of the building and the lives of people.

(ii) To the energy demand and the well-being of the users of the building. In case of a bad state, the building materials lose their thermal capacity, which leads to a reduction of the energy efficiency level of the building and to a reduction of the thermal comfort control of each room of the building.

Therefore, it is fundamental to address the continuous deterioration of the structures of buildings due to the appearance of different anomalies caused by aging, unforeseen events, environmental conditions and previous incorrect restoration treatments. This includes inspecting the building design to identify, for example, wall layers with incorrect thickness according to the regulations. Documentation of the position and nature of possible hidden targets or hidden structural elements of the building is also included for condition assessment and intervention [5]. For that, ISO standards recommend the use of non-destructive techniques (NDTs) as inspection tools for both a punctual and prolonged study over time, regardless of the nature of the building and the anomaly [6]. NDTs improve safety, sustainability, and durability in the building sector due to their lower subjectivity and faster inspection speed compared to traditional inspection tools [7], and non-intrusive and non-damaging to building integrity compared to destructive inspection tools [8].

NDTs allow the analysis with a high level of detail in any building, providing a wide range of knowledge of the structure under study. This is demonstrated by the recently published reviews on:

(i) the condition evaluation of various historic monuments constructed of stone, brick masonry, or reinforced cement concrete [9].

(ii) the building envelope diagnostics for standardized energy audits [10].

(iii) the traditional procedures and futures perspectives of NDTs for the diagnosis of heritage buildings [11].

In this review article, a compilation of the state-of-the-art of application of InfraRed Thermography (IRT) and Ground-Penetrating Radar (GPR) for building assessment is performed, with special emphasis on applications that integrate both technologies. These techniques are selected due to their technological maturity and their wide use as inspection tools in the building sector. However, to the best knowledge of the authors, it is the first time that a joint compilation of the state-of-the-art of both IRT and GPR for building evaluation is performed in the same work, especially in the compilation of applications that integrate both NDTs. Then, the objective of this work is to demonstrate the high capabilities of these two NDTs in inspecting the design of a building, documenting its internal structure and identifying both surface and subsurface anomalies, both individually and together, and even with other NDTs. In this way, another objective is to highlight the benefits in complementarity of information and validation of results by combining both inspection tools. With this purpose, Section 2 briefly describes the performance of each technology, through their comparison and analyzing their individual and common advantages for building inspections. Next, Section 3 describes the methodology performed in the review process and Section 4 compiles the state-of-the-art IRT and GPR applications divided into three sub-sections: structural safety (Section 4.1), energy efficiency and user well-being (Section 4.2), and heritage preservation (Section 4.3). The same structure is applied for each sub-section: representation both in text and table of the most common applications according to the corresponding objective, annexing the most relevant works by means of referencing, the building materials studied, and the NDT or NDTs used. Section 5 presents three different case studies, with the aim of illustrating the potential of the combined use of IRT and GPR in building assessment from different perspectives: structural safety, energy efficiency and user well-being, and heritage prevention. Finally, Section 6 covers the final remarks after the analysis of the previous sections and describes the future perspectives of the IRT and GPR inspection in buildings.

2. Brief Description and Comparison of IRT and GPR

IRT uses an InfraRed (IR) camera to measure and analyze a thermal pattern based on the principle that all bodies at a temperature above absolute zero (0 K/−273.15°C) emit electromagnetic radiation. Since 0 K/−273.15°C is an unattainable limit according to the third principle of thermodynamics, all bodies are measurable with an IR camera. The electromagnetic radiation emitted by a body is detected by the IR camera and transformed into an electronic signal by means of a set of photoelectric sensors that form a plane array inside the camera. Then, electronic signal is processed to produce a thermal image based on Planck's [12] and Stefan-Boltzmann's [13] Laws. Specifically, an IR camera allows the entrance through the lens of radiation emitted by the body in one of the sub-bands of the IR spectrum. The choice of the IR spectrum among all the bands of the electromagnetic spectrum is because the maximum radiation intensity emitted by a body is located in this wavelength interval, according to Wien's displacement law [13]. When the body is under normal temperature conditions, the narrow portion of the IR spectrum is between 8 and 15 μm (20–37 THz), that is, the IR spectrum sub-band of Long-Wave InfraRed (LWIR), is the optimal sub-band to measure the thermal state of the body. In addition, the atmospheric absorption level (atmospheric attenuation) of the radiation emitted by the body is low in this IR sub-band, allowing more radiation to reach the IR camera lens [14].

Heat transfer is understood as an exchange of thermal energy between a high-temperature medium to a low-temperature medium. This process of heat propagation in different media explains the abnormal surface temperature

Table 1: Comparison between IRT and GPR techniques. Adapted from [18].

Advantages of IRT over GPR	Advantages of GPR over IRT	Common advantages
Non-contact tool although ground-coupled antennas can operate with a separation of 2–5 cm from the surface, and GPR antennas are operating in a non-contact mode (air-coupled antennas)	Lower dependence on the environmental conditions although it is highly influenced by the subsurface materials	Evaluation of the properties of the body without causing damage since they are NDTs
Ability to analyze any surface regardless of the type of material, since metal surfaces are not penetrated by the radar waves	Independence of the thermal condition of the surface under study and of surface parameters for a correct reading	Possibility to perform large-scale studies of materials in real time
More ability to cover more surface under study in less time	Long-range depth analysis (from 1 cm to 10 m depending on the frequency) over a couple of centimeters with active IRT	Repeatable and reliable tools, high maneuverability

patterns of a body. The three mechanisms of heat transfer are conduction, convection, and radiation. When dealing with transient thermal problems and building inspection using IR cameras, conduction is the most important mode of heat transfer, as this mechanism defines the transfer of thermal energy between solid bodies, and consequently their emission of radiation. Materials conduct heat at different rates, and these rates are related to their thermal properties. These properties are different between surface and internal anomalies with respect to the sound volume of the body. Thus, it is possible to make the identification of internal anomalies (qualitative analysis), and their thermal characterization and depth estimation (quantitative analysis), from the application of processing algorithms to the thermal images captured with the IR camera [15]. When the analysis of surface anomalies is the objective, their thermal footprints are detectable with thermal transient states caused by solar radiation (passive IRT). However, thermal excitation with higher intensity than solar radiation is necessary to reach the thermal footprint of internal anomalies to the surface of the body, using artificial thermal sources (flash and halogen lamps, hot and cold air guns, electrical heating, ultrasonic excitation, eddy currents, microwaves, and others) (active IRT) [16].

The GPR method uses ElectroMagnetic (EM) waves (from 10 to 6000 MHz, belonging to the radio spectrum) to acquire information from the subsurface. A transmitting antenna generates the EM wave that is propagated through the media under study. The wave is partially reflected when encountering a discontinuity in the dielectric properties of media and recorded at the surface by a receiving antenna, while the other part of the signal continues to propagate until reaching the total time window set. The intensity or strength of the reflected signals, typically called amplitude, is proportional to the dielectric contrast value between two different media. As a result, an XZ image (radargram) is obtained as a result of the GPR analysis. The values of the radargram represent the amplitude values of the different reflected signals, which are measured as the transmitting antenna moves along the surface under study. Thus, the X axis represents the distance (meters) of each trace (position of each echo received) and the Z axis represents the two-way travel time of the echoes through the media. If the time required to propagate to a reflector and back is measured, and the velocity of the signal propagation through media is known, the depth of the reflectors can therefore be determined. A deep theoretical background can be found in [17].

Table 1 shows a comparison between IRT and GPR techniques, indicating the advantages of one technique over the other in columns 1 and 2; and the common advantages of both when inspecting a body in column 3.

3. Methodology

This review article focuses on the integration between IRT and GPR for building assessments. The main criteria considered in the search method were:

(i) The use of Scopus and Google Scholar databases to retrieve the related research publications. A set of keywords was used for the search. These always included the terms IRT and GPR, together with one of the objectives to be achieved in building assessment, objectives defined in the Introduction section ("structural safety," "energy efficiency and user well-being," "heritage preservation") and the term building, in order to cover a wide area of different applications.

(ii) The consideration of books, conference papers, technical notes, and manuscripts such as review articles and original research, when they matched the search criteria. Then, the redundant or irrelevant publications were excluded from the initial review list based on reading the title and abstract of each publication. Journal articles were preferred to conference publications when they addressed similar topics, and experimental data were preferred to simulated data. Original research and case study articles were preferred to review articles, especially those indexed in the Journal Citation Reports (JCR) database.

(iii) After that, publications that were inaccessible to the reviewers were excluded from the review list. Apart from Open Access articles (most from MDPI), the institutional publishers available and most selected were Elsevier, Springer, and Taylor & Francis.

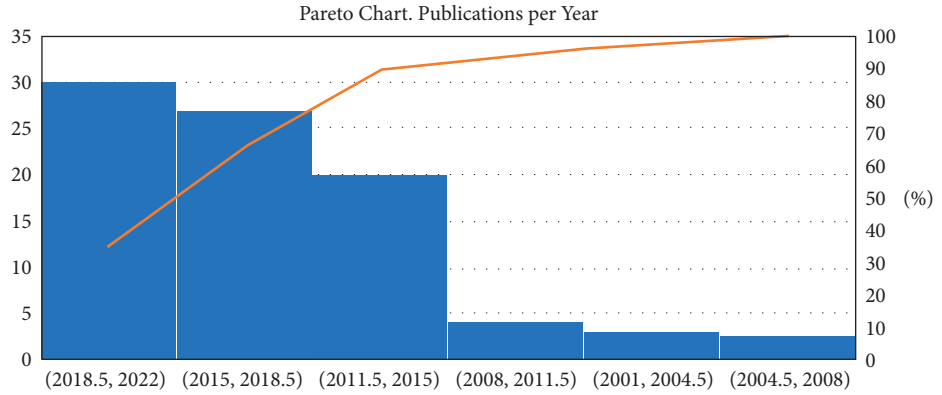

Figure 1: Number of related publications reviewed in this work (99 selections) per year since 2000.

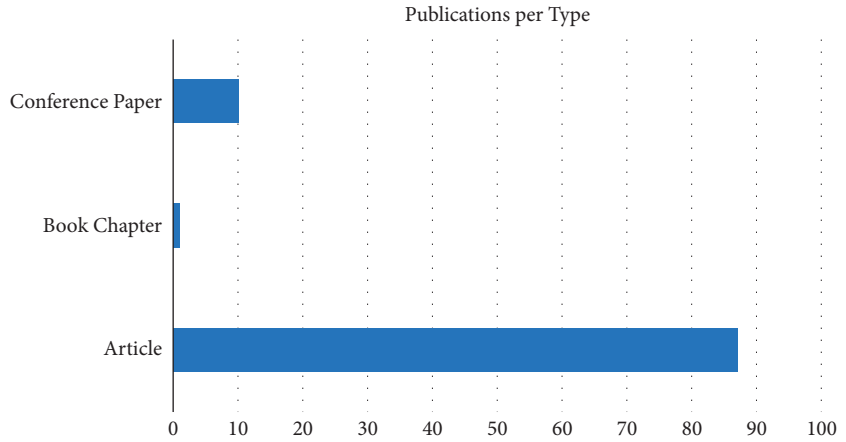

Figure 2: Publications reviewed in this work are categorized by their typologies.

(iv) 99 publications were relevant to the review topic. Based on these, the applications made for each of the objectives in the evaluation of buildings have been broken down into different groups, making groups by affinity. After that, the type of material studied has been analyzed for each reference, together with an evaluation of whether the IRT-GPR integration has taken place and whether other NDTs have been used in addition.

Studies combining IRT and GPR for building assessment have shown an exponential increase in interest since 2000. Figure 1 shows the number of publications relevant to this review topic per year since 2000. Most were published since 2015, with a substantial jump from previous years, with 7–8 publications per year since 2018. Most of the publications reviewed were articles, with 87 publications (87.9%), followed by conference papers and book chapters with 10 (9.9%) and 2 (2.2%) publications, respectively, as shown in Figure 2. Regarding the number of publications per objective, an equal distribution has been found over the years, with 32% in

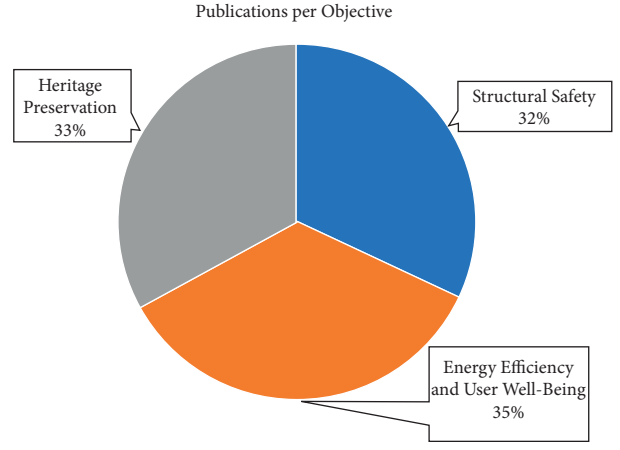

Figure 3: Number of publications reviewed that address each objective established in the building assessment.

Table 2: Summary table of the state-of-the-art of IRT and GPR techniques applied to structural safety application in the building sector.

Application	Materials	IRT	GPR	Other NDTs	References
Detection of hidden targets or structural elements (tension cables, grade beams, conduits)	Hidden wiring control under the most common cladding materials: drywall, PVC lining boards, ceiling and chipboard panels	✓			Petrosyants [19]
	Existence of corridors under the building		✓		Núñez-Nieto et al. [20]; Pérez-Gracia et al. [21]
	Supporting structures (floor)		✓		Pérez-Gracia et al. [21]
	Post-tensioned cables (concrete slab) (servicing a manufacturing facility)		✓		Gehrig et al. [22]
Identification of concrete degradation	Concrete structures externally reinforced with fiber reinforced polymer (FRP) composites	✓			Yumnam et al. [23]
	Reinforced concrete (floor)		✓		Lorenzo et al. [24]
Detection of cracks, fractures, and voids	Mortar board, extrapolated to building scale	✓			Bauer et al. [25]
	Masonry façade with ceramic tile	✓			Bauer et al. [26]
	Steel fiber-reinforced concrete	✓		Ultrasonic Rayleigh waves	Aggelis et al. [27]
	Masonry made of bricks and tuff, and reinforced with a thin high-strength and high-conductive fibre fabric		✓	Electrical resistivity tomography (ERT)	De Donno et al. [28]
	Sack masonry wall (made of a calcareous natural stone called "pietra leccese" and "tuffo" blocks)		✓		Negri and Aiello [29]
	Travertine panel (with a mortar layer)		✓		Leucci et al. [30]
	Reinforced concrete		✓		Gehrig et al. [22]; Pérez-Gracia et al. [31]; Bavusi et al. [32]
	Limestone walls (wine cellar buildings)		✓	Terrestrial laser scanning	Villarino et al. [33]
Detection of delamination and detachments	Plastered three-leaf stone masonry walls	✓	✓		Cotič et al. [34]
	Concrete structures	✓			Cotič et al. [35]
	Mortar board, extrapolated to building scale	✓			Bauer et al. [25]
	White ceramic tiles and colored ceramic tiles	✓			Lourenço et al. [36]; Garrido et al. [37]
	Plastered walls	✓			Barreira et al. [38]
Detection and localization of rebar	Reinforced concrete structures	✓			Keo et al. [39]
		✓		Eddy current technique	Szymanik et al. [40]
	Concrete components (wall, column, beam, and floor of the buildings)		✓	Microwave tomography, ElectroMagnetic induction (EMI)	Pérez-Gracia et al. [31]; Bavusi et al. [32]; Pérez-Gracia et al. [21]; Zhou et al. [41]; Xiang et al. [42]; Liu et al. [43]; Xiang et al. [44]
	Reinforced concrete (RC) pavement (servicing a manufacturing facility)		✓		Gehrig et al. [22]
	Reinforced concrete column beyond a double wall of hollow bricks		✓		De Domenico et al. [45]

Table 2: Continued.

Application	Materials	IRT	GPR	Other NDTs	References
Detection of rebar corrosion	Reinforced concrete (inner roof surface of a military battery)	✓	✓		Solla et al. [46]
	Epoxy coated and uncoated rebar in concrete	✓			Baek et al. [47]; Na and Paik [48]; Goffin et al. [49]
	Reinforced concrete (floors and curtain walls)		✓		Núñez-Nieto et al. [20]; Taştan et al. [50]
	Concrete slabs (underground parking garage)		✓		Dinh et al. [51]
Monitoring of subsidence and settlement phenomenon (floors and façade panels contain cracks)	Shallow foundations (precast (RC) buildings)		✓	ERT and geotechnical drillings	Capozzoli et al. [52]
	Heavy loaded RC pavement servicing a manufacturing facility		✓	Geotechnical studies (dynamic probing super heavy (DPSH) and standard penetration test (SPT) tests)	Solla et al. [53]

structural safety, with 35% in energy efficiency and user well-being, and with 33% in heritage preservation, respectively, as shown in Figure 3.

4. Applications of IRT and GPR in Building Assessment

4.1. Structural Safety. Good structural health is of vital importance for a building to be able to provide its performance to the user in optimal conditions. Among the requirements to be met, there is one common to all buildings, that is, safety. For that, it is essential to know the condition of each building material before a collapse of the structure happens, including factors such as the age of the material and its constitution, as well as possible existing anomalies. Given the scope of IRT and GPR, both technologies are able to provide both structural information of the building and identification of critical areas, mainly:

(i) The estimation of the position of hidden targets or structural elements, such as tension cables, grade beams, conduits.

(ii) The analysis of the degradation rate.

(iii) The detection of cracks, fractures, and voids.

(iv) The identification of delamination and detachment.

(v) The estimation of the position of rebars and the study of their corrosion states.

(vi) The monitoring of subsidence and settlement phenomenon.

As evidence of the applicability of IRT and GPR, a summary table (Table 2) of the state-of-the-art is shown below.

4.2. Energy Efficiency and Well-Being. Energy conservation in the building sector is a fundamental aspect when it comes to mitigating the advance of global warming, which directly leads to an economic reduction of the energy bill and a better quality of life for users. A better well-being of the users of a building with high efficiency in terms of energy as it leads to a higher stability of thermal comfort. There are three factors to be considered in a building envelope: its thickness, its thermal mapping, and its overall heat transfer coefficient, known as U-value. These factors are good indicators of the level of energy efficiency and thermal comfort of a building, being interrelated:

(i) The thickness of the construction materials is a fundamental parameter in establishing an adequate thermal inertia of the building envelope.

(ii) The thermal mapping allows for to identify possible anomalies in the building envelope, such as any malfunction of the Heating, Ventilation, and Air Conditioning (HVAC) system integrated in the building. Thermal mapping also allows the identification of the following three anomalies, which are the most common and the most detrimental in the building sector in terms of energy efficiency and well-being: moisture, thermal bridges, and air infiltration.

(iii) The U-value takes into account not only the thickness of the building materials (geometrical properties), but also the thermophysical properties, evaluating more precisely the thermal resistance of a building envelope to heat transfer between the interior and the exterior.

GPR and IRT can successfully address each point described above, especially IRT because temperature measurement is more related to the subject matter of this section as opposed to the radio EM wave measurement, with applicability to a wide range of materials. A summary table (Table 3) of the state-of-the-art is shown below.

4.3. Heritage Preservation. The protection and management of cultural heritage must be particularly cautious with the preservation of its singular and historical character. IRT and GPR have also been widely used for preventive damage detection and heritage preservation. Within cultural heritage, these techniques have been successfully applied to inspect monumental buildings, statues, frescoes, and mosaics, among others. In this context, these techniques proved to be effective in obtaining valuable information, mainly including:

Table 3: Summary table of the state-of-the-art of IRT and GPR techniques applied to energy and well-being conservation in the building sector.

Application	Materials	IRT	GPR	Other NDTs	References
Estimation of thickness	Two-layered thermally thin structure	✓			Jena and Gupta [54]
	Reinforced concrete base (slab; foundation floor)		✓		Gehrig et al. [22]; Pérez-Gracia et al. [31]; Núñez-Nieto et al. [20]
	Casted concrete with embedded rebars		✓	EMI	Zhou et al. [41]
	Hollow bricks (wall)		✓		De Domenico et al. [45]; Pérez-Gracia et al. [21]
	Metal and wooden beams (roof)		✓		Pérez-Gracia et al. [21]
	Limestone walls (wine cellar buildings)		✓	Terrestrial laser scanning	Villarino et al. [33]
Inspection of the heating, ventilation, and air conditioning (HVAC) system	Tiling coating and parquet	✓	✓		Lagüela et al. [55]
Detection of moisture	Masonry wall (brick & stone)	✓	✓		Garrido et al. [18]
	White plaster walls in different buildings (indoor) and a concrete building façade (outdoor)	✓			Garrido et al. [56]
	White ceramic tiles and colored ceramic tiles	✓			Lourenço et al. [36]; Garrido et al. [37]
	Adhered ceramic building façades	✓		Surface moisture meter	Edis et al. [57]
	Different parts of buildings, both from inside (plaster) and outside (concrete)	✓			Garrido et al. [58]
	Tuff bricks wall		✓	Laser scanning	Agliata et al. [59]
	Reinforced concrete		✓		Pérez-Gracia et al. [31]
Detection of thermal bridges	From semi-detached two-story brick buildings, to five-story self-standing brick buildings	✓		Photogrammetry	Garrido et al. [60]
	Controlled test chamber	✓			O'Grady et al. [61, 62]; Baldinelli et al. [63]
	Brick building façade	✓			Sfarra et al. [64]; Kim et al. [65]
	Different parts of buildings, both from inside (plaster) and outside (concrete)	✓			Garrido et al. [58]
	Rendered brick façade and vibrated concrete rough block façade	✓		Photogrammetry	Antón and Amaro-Mellado [66]
Estimation of U-value	Single-leaf brick and mortar walls and multi-leaf brick and mortar walls	✓		Heat flux meter	Tejedor et al. [67]
	Thick massive laminated spruce timber walls with different thicknesses	✓		Heat flux meter	Danielski and Fröling [68]
	Timber (light) and brick (heavy) structures	✓		Heat flux meter	Albatici et al. [69]
	Building rooftops	✓		Heat flux meter	Patel et al. [70]
	Insulated wood-framed wall assemblies	✓			Mahmoodzadeh et al. [71]
	Single-leaf lightweight concrete walls and heavy lightweight concrete multi-leaf walls	✓		Heat flux meter	Tejedor et al. [72]
	Brick building	✓		Laser scanning	Lagüela et al. [73]
	Concrete building, and glass and wood building	✓		Laser scanning, photogrammetry	González-Aguilera et al. [74]
	Building with lightweight material	✓		Photogrammetry	Natephra et al. [75]

Table 3: Continued.

Application	Materials	IRT	GPR	Other NDTs	References
Detection of air infiltration	A room with plaster walls of a residential multi-story building	✓		Blower door test	Lerma et al. [76]
	An office with plaster walls of a three-story building	✓		Blower door test	Barreira et al. [77]
		✓		Photoacoustic gas analyzer	Liu et al. [78]
	Timber-framed building envelope joints	✓		Blower door test	Kalamees et al. [79]
	Controlled test chamber	✓			Gil-Valverde et al. [80]; Royuela-del-Val et al. [81]

(i) The detection of damage in façades or walls, such as delamination, fractures, cracks, detachments, and moisture.

(ii) The investigation of the conservation state of timber beams in floor and ceiling systems, and the structural integrity of basement, wall foundation, floors, and soil systems.

(iii) The evaluation of the internal structure and defects in structural elements or columns, and decorative elements.

(iv) The inspection of the state of conservation of walls and works of art, such as the adhesion between different layers and moisture in paintings and frescoes, or stratigraphy and water content in mosaics.

A summary table (Table 4) of the state-of-the-art is shown below.

5. Case Studies

5.1. Structural Safety: Detection of Corrosion in Structures. This case study presents the use of GPR and IRT for the detection and evaluation of corrosion in old construction, where the corrosion can lead to the collapse of the structure. In this case, the combination of techniques allows differentiating between corroded areas and areas affected by moisture, as well as to identify damages in the interior of the structure such as cracking and debonding.

The construction under study is a Military Base, located at the coast in the North of Spain (at 200 m distance from the sea), and dates from the 30 s of the XXI century. This location explains that corrosion is the main threat to the stability of the structure. More information about the site can be found in [46], and its interior can be seen in Figure 4.

5.1.1. Methodologies. The GPR survey was conducted using a ProEx GPR system with a 2.3 GHz antenna. The profile lines were acquired through the ceiling of the structure which consists of a reinforced concrete slab (see Figure 4). Data collection was carried out by moving the antenna perpendicular to the direction of the rebar, using the setting parameters: 1 cm spatial sampling and time window of 14 ns (composed of 292 samples per trace). Before interpretation, the 2D radargrams produced were processed in the ReflexW software to suppress the continuous component (Subtract-DC-Shift), to amplify the received signals (Gain function), to remove horizontal continuous low-frequency reflectors (Subtracting average), and to remove both low- and high-frequency noise (Butterworth) in both 1D and 2D dimensions.

Regarding the thermographic inspection, a camera NEC TH9260 was used. The inspection distance between the camera and the walls of the Military Battery was 1 meter, in such a way that the Field of View was 21.7° horizontal and 16.4° vertical. Emissivity is set to 1, in order to make non-compensated temperature measurements of apparent temperature. This mode is selected because of the variety of materials present in the surface of the walls of the battery, which would result in multiple emissivity values to compensate. Atmospheric attenuation was compensated, considering the ambient conditions: 16°C and 70% relative humidity. The temperature profiles measured along the GPR profiles were analyzed and filtered with the aim of detecting and delimiting the pathologies present.

5.1.2. Results and Findings. Observing Figure 5, the GPR data produced allowed for the identification of the following pathologies:

(i) Moisture content was detected as the travel-time distance increased because the velocity of propagation of the signal in water is lower.

(ii) Higher mineral salts content was interpreted in zones with severe absorption of the signals (or signal attenuation).

(iii) Detachment and voids beneath detached concrete were identified as hyperbolic reflections (rebar) near the surface because of the faster velocity of propagation of the radar signal in air, while showing higher amplitude spectrum (strong reflections).

(iv) Fissuration was interpreted as signal scattering (diffractions).

The evaluation of the thermographic images shows that moisture is an important factor in the walls of the battery, which covers the effect of any other pathologies that could be present. In this case, since the apparent temperature was measured, it is important to consider that some thermal anomalies can be provoked by different emissivity materials. Consequently, the emissivity factor is considered as a

Table 4: Summary table of the state-of-the-art of IRT and GPR techniques applied to cultural heritage buildings.

Application	Materials	IRT	GPR	Other NDTs	References
Estimation of thickness and quality of walls	Limestone	✓	✓	Laser scanning, aerial surveying	Solla et al. [82]
	Stone building façade	✓		Ultrasonic technique	Diana and Fais [83]
	Brick wall covered with marble		✓	Ultrasonic pulse velocity (UPV)	Yalçıner et al. [84]
	Limestone		✓	Seismic tomography	Pérez-Gracia et al. [85]
	Masonry walls		✓		Rasol et al. [86]
	Masonry of bricks		✓		Cintra et al. [87]
Detection of hidden targets or structural elements	Two-story houses with gabled roofs, masonry brick, and stucco	✓			Glavaš et al. [88]
	Small pieces of roughed-hewn stones to build masonry and calcareous materials	✓			Sfarra et al. [89]
	Stone and plaster walls	✓			Ibarra-Castanedo et al. [90]
	Stones walls		✓	Laser scanning	Santos-Assunçao et al. [91]
	Masonry of bricks		✓		Cintra et al. [87]
Detection of delamination, cracking and cavities in walls/ façade and columns	Lime plaster base with a thin layer of visible stucco marble	✓			Arndt [92]
	Plaster layer over a support of marble, tuff with plaster	✓		Geophysical techniques	Carlomagno et al. [93]
	Small pieces of roughed-hewn stones to build masonry and calcareous materials	✓			Sfarra et al. [89]
	Stone and plaster walls	✓			Ibarra-Castanedo et al. [90]
	Brick wall covered with marble		✓	UPV	Yalçıner et al. [84]
	Rubble filled stone walls		✓		Johnston et al. [94]
	Limestone		✓	Seismic tomography	Pérez-Gracia et al. [85]
	Masonry walls		✓	Ultrasonic and flat-jack test	Guadagnuolo et al. [95]
	Plastered and painted		✓		Işık et al. [96]
	Stone and brick walls		✓	Microwave tomography	Catapano et al. [97]
Detection of moisture in façade, walls, columns, and pavements	Granite, bricks and limestone	✓	✓	Electrical conductivity meter (EC), relative humidity (RH)/temperature (T) monitoring by means of data loggers (DL), wireless sensor networks (WSN)	Martínez-Garrido et al. [98]
	Masonry façade	✓	✓	Laser leveling (LL), ambient vibration testing (AVT)	Diz-Mellado et al. [99]
	Brick wall and concrete wall	✓			Garrido et al. [100]
	Two-story houses with gabled roofs, masonry brick and stucco	✓			Glavaš et al. [88]
	Marble, granite, and breccias		✓	Microclimatic investigation	Cataldo et al. [101]
	Plastered and painted walls and dome		✓		Işık et al. [96]
	Rough stone building	✓		Laser scanning	Nardi et al. [102]

Table 4: Continued.

Application	Materials	IRT	GPR	Other NDTs	References
Detection of moisture and detachment behind mosaics, marquetries, paintings, statues, and frescoes	Frescoed wall	✓	✓	Structure-from-motion photogrammetry (SfM)	Danese et al. [103]
	Mural paintings (frescoes)	✓			Cadelano et al. [104]
	Wall paintings	✓			Mouhoubi et al. [105]
	Tessellatum mosaic	✓			Garrido et al. [106]
	Wooden marqueterie	✓			Chulkov et al. [107]; Garrido et al. [108]
	Covered walls made of bricks		✓	UPV	Yalçıner et al. [84]
	Tesserae mosaic pavement		✓		Calia et al. [109]
	Marble statue	✓		Laser scanning	Campione et al. [110]
Study of the structural integrity of wall foundation, floors, and soil system (zonification, cavities, subsidence, etc.)	Masonry façade	✓	✓	LL, AVT	Diz-Mellado et al. [99]
	First case: natural and anthropic filling Second case: loose alluvial and pyroclastic soils		✓	Electrical ResisTivity (ERT)	Evangelista et al. [111]
	Stone-block walls		✓	ElectroStatic (ES) quadrupole test	Dabas et al. [112]
	Alluvial soil		✓	Ultrasonic and flat-jack test	Guadagnuolo et al. [95]
	Reinforced concrete floor		✓		Işık et al. [96]
	Floor layers: stone tiles, reinforced concrete screed, floor heating, thermal insulation, cross-reinforced concrete slab, sand backfill		✓		Rucka et al. [113]
Inspection of timber floor/ ceiling and location of beams	Wooden	✓			Martínez and Martínez [114]
	Wooden		✓	Drilling and penetration resistance, accelerometers for seismic measurements	Fontul et al. [115]
Inspection of basement	Brick and plaster masonry	✓		Capacitive moisture meter	Balík et al. [116]
	Basement roof supported by cast-iron columns (reinforced bars)		✓		González-Drigo et al. [117]
	Almost flat rooftop with interior vaults and columns		✓		Rasol et al. [86]

Figure 4: Interior of the military base in Cabo Udra, greatly affected by moisture and vegetation that can cause the corrosion of the metallic structure.

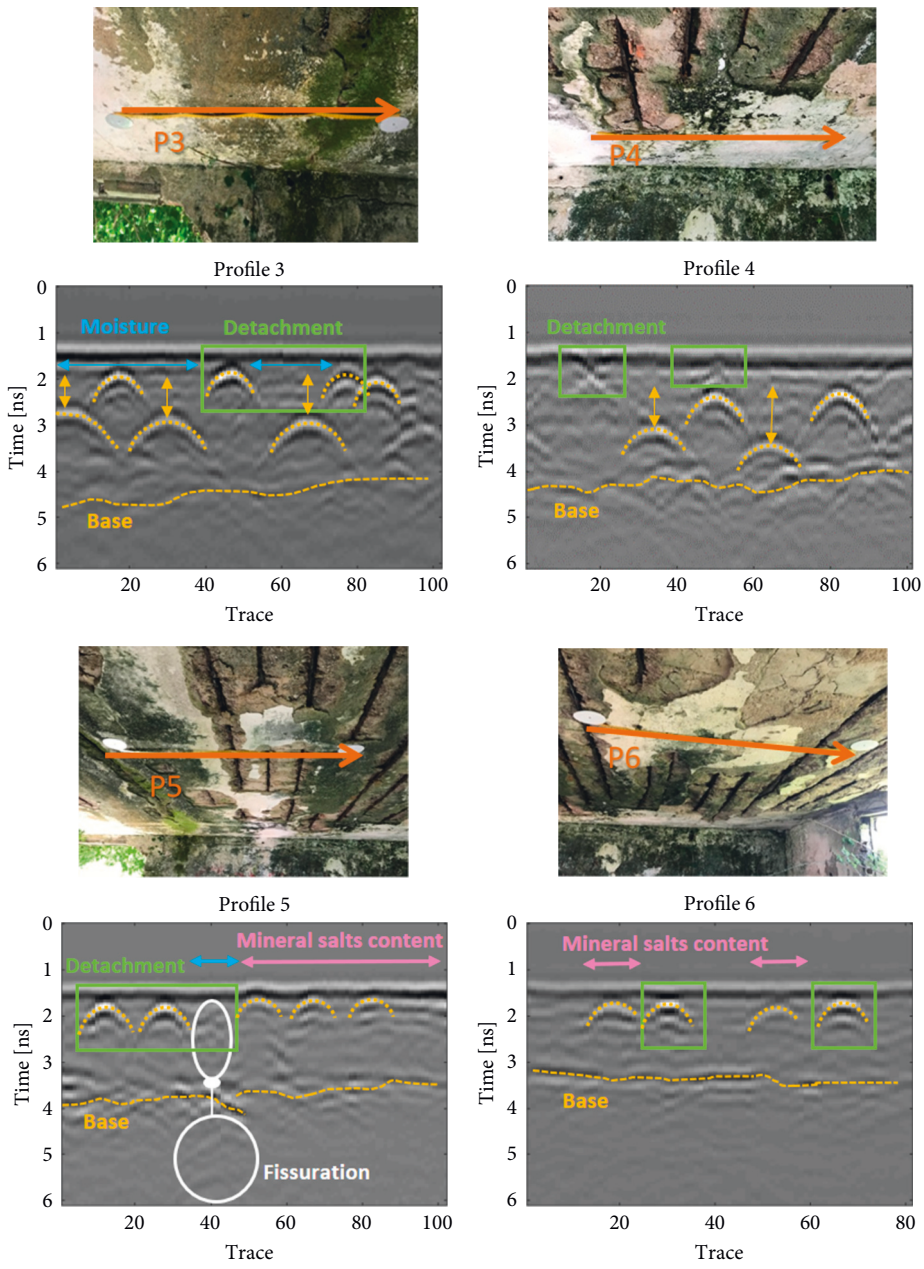

Figure 5: GPR results showing the interpretation of the pathologies identified (modified from [46]).

parameter for evaluation, in order to determine the type of each pathology: as an example, moisture appears as an area with a different temperature than dry materials, but the temperature transition is continuous; while mineral salts also present different temperature, but because it is caused by a difference in emissivity, the temperature transition is sharp. These effects can be seen in Figure 6, where different profiles, their thermographic images and their temperature profiles with identification of pathologies are shown.

In this particular application, the combination of GPR and IRT techniques was applied to confirm the interpretation of pathologies made by each technique independently, and IRT was useful to explain some signal scattering occurring in the GPR signal: the reason for the scattering was located in the presence of moisture and mineral salts, and the possibility of failure by the GPR antenna was dismissed.

5.2. Energy Efficiency and Well-Being: Detection of Building Installations (Radiant Heating Floor). This case study presents a combined use of GPR and IRT for the evaluation and characterization of thermal floors in residential buildings. The test site corresponds to a joint kitchen and living room, with low-reflectivity ceramic tiles as floor coating (see Figure 7).

5.2.1. Methodologies. A ProEx GPR system was used, with a 2.3 GHz antenna. The setting parameters used were a 2 cm

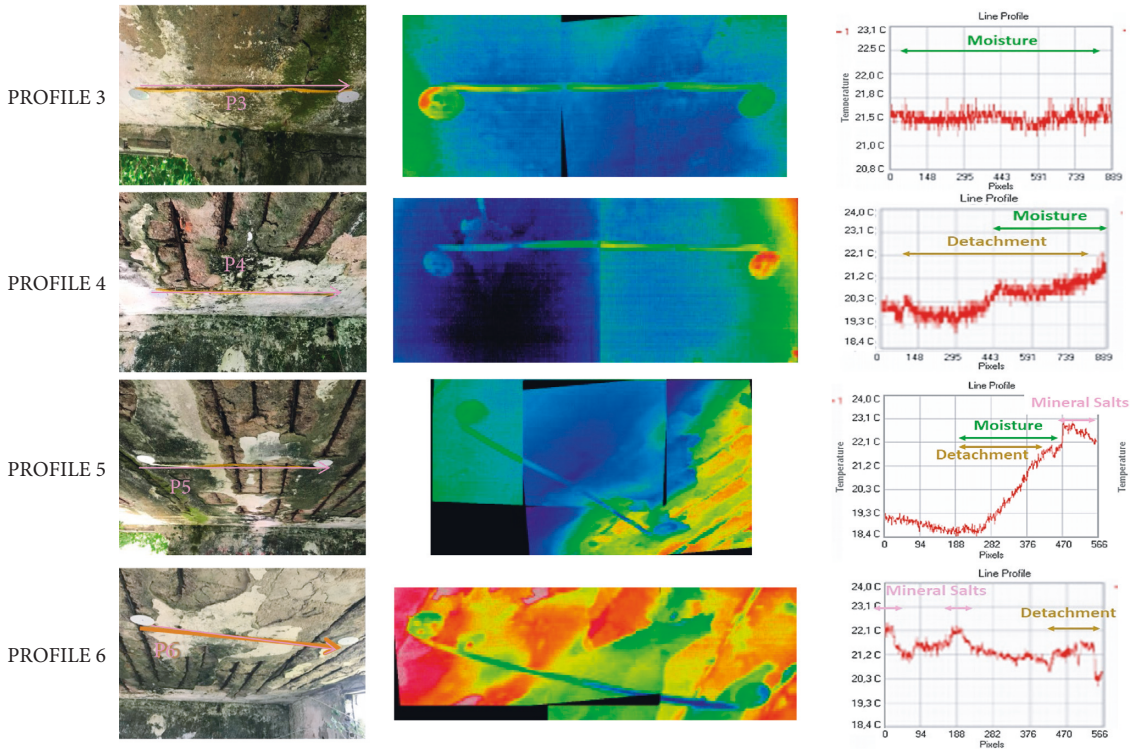

Figure 6: Results of the pathologies detected during the thermographic inspection in the areas coinciding with 4 GPR profiles. Temperature and emissivity anomalies are considered for the identification of pathologies: moisture, detachment, and mineral salts (modified from [46]).

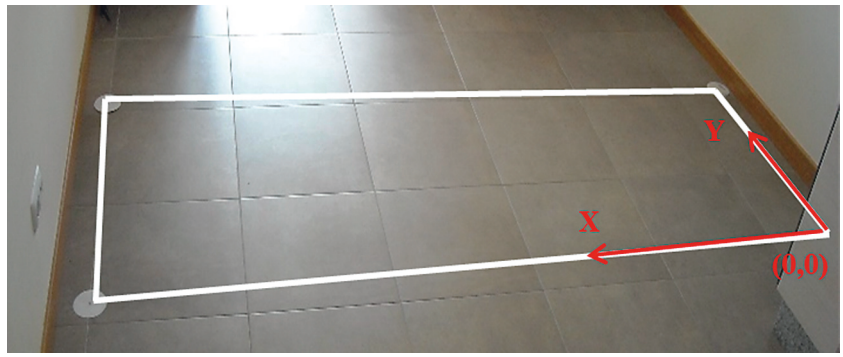

Figure 7: Picture of the test site showing the prospected grid (modified from [55]).

spatial sampling and a 12 ns time window. An encoder-based wheel was attached to the antenna, as a distance measurement instrument, to measure the profile length and to control the spatial sampling. A 3D data acquisition was conducted with equidistant parallel profile lines at regular intervals of 5 cm. The profile lines were collected with the antenna polarization orthogonal to the longitudinal direction of the heating pipelines. Both the 2D radargrams produced and the 3D cube were processed in the ReflexW software.

The thermographic camera used was an NEC TH9260 camera, with an Uncooled Focal Plane Array (UFPA) with a size of 640×480, a precision of 0.2°C and a thermal resolution of 0.1°C. Images were acquired with an emissivity value of 1, in such a way that apparent temperature is measured toward a qualitative analysis of the performance of the radiant heating system. In addition, in order to minimize the appearance of reflected radiation, images were acquired from a point of view with an inclination of 10° from perpendicular to the floor, and at a distance of 2 meters for an optimal image field of view.

5.2.2. Results and Findings. GPR provided information about the number of pipelines and distribution. As shown in Figure 8(a), GPR data revealed the presence of three pipelines.

The thermographic mosaic showed the presence of two pipelines (Figure 8(b)). The spatial correspondence between the 3D GPR image and thermographic mosaic leads to the conclusion that the central pipeline is not working.

Comparing both techniques, GPR gives information about all pipelines but cannot distinguish whether they are

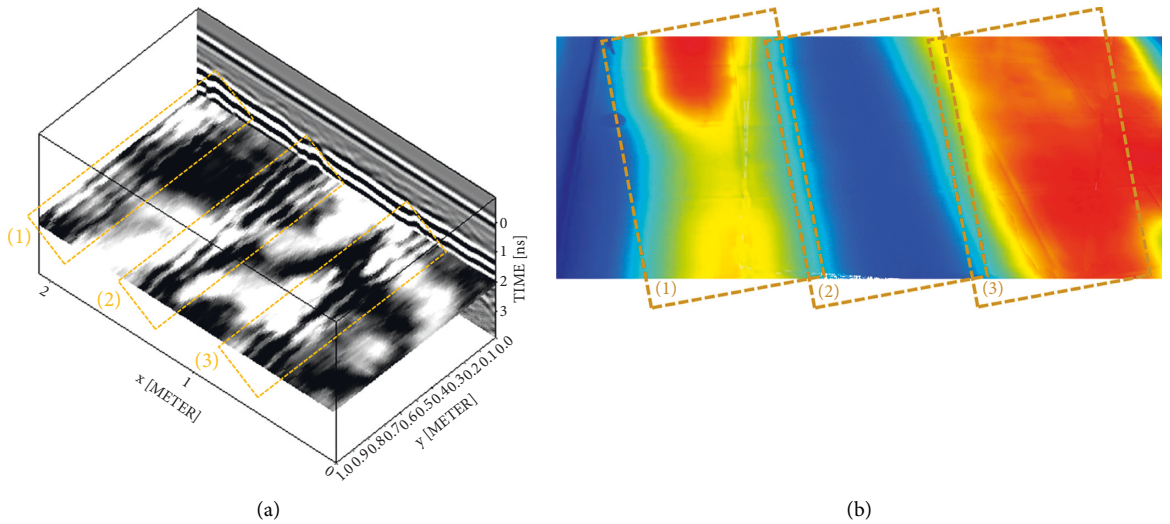

(a) (b)

FIGURE 8: GPR results (a) showing the existence of three pipes, while IRT results (b) show the functioning of only two pipes. The conjoint study allows detecting the failure in performance of one of the pipes in the radiant heating system (modified from [55]).

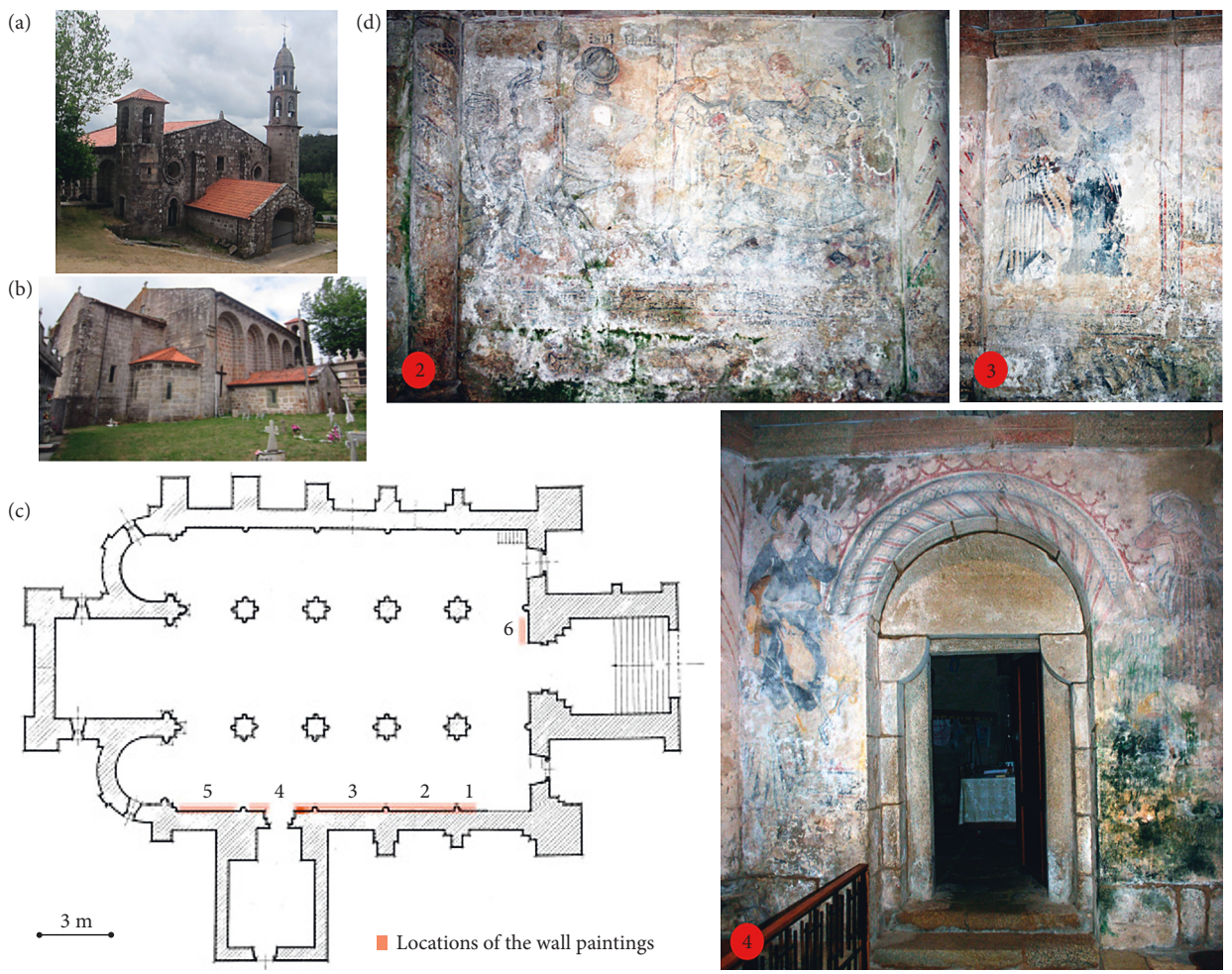

FIGURE 9: General view of the San Julián de Moraime Church (a), northern wall (b), plant view of the interior and locations of the wall paintings (c), and some of the paintings showing deterioration (d).

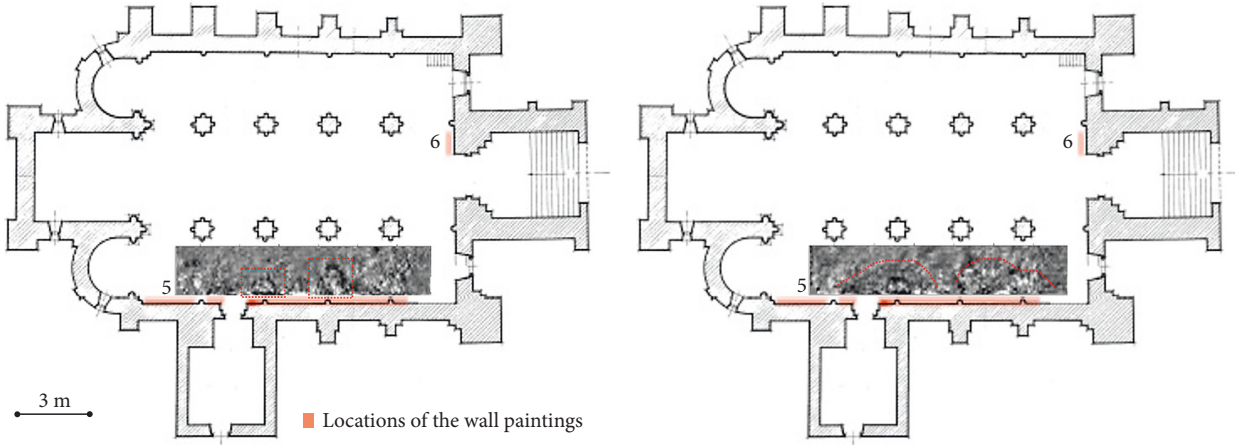

Figure 10: 3D GPR imaging: time-slices at depths of 50 cm (a), and 60 cm (b).

working or not. IRT can detect only the working installations. Moreover, the different thermal print between the pipelines on the left and on the right shows a malfunctioning of the pipeline on the left, given its colder temperature distribution.

5.3. Heritage Preservation: Moisture Detection in San Julián de Moraime Church (Muxía, NW Spain). This Church, which was declared an Asset of Cultural Interest in 1972, has more than 46 m2 of medieval wall paintings. As shown in Figure 9, these paintings are located in five sections through the northern wall, and represent the seven capital sins: section 1—sacred form, section 2—the pride and the greed, section 3—the anger and the lust, section 4—the gluttony and the envy, section 5–the sloth and the death. There are visible signs of deterioration such as moisture, presence of fungi and algae, saline efflorescence (chlorides, sulfates, nitrates, and nitrites), calcareous formations by carbonation, and dissolution of pigments. The main factors contributing to this deterioration are: (i) moisture, which multiple origins (moisture by capillarity and infiltration, residual moisture, and moisture caused by condensation); (ii) climatic conditions (the site of Moraime has a wet and warm weather during all the year with a maximum temperature of 11° and 20°C in winter and summer, respectively); (iii) presence of marine aerosols given its proximity to the coast; (iv) the interior of the Church is below the ground level; and (v) the northern wall is the least sunny and ventilated, coinciding with the drainage ditches of the rainwater. This situation mainly affects the first three sections. Section 4 gives to the Sacristy, which provides isolation from the outside, however, the contact with the corresponding buttresses implies entry of moisture. In the last section, the outer wall coincides with a flat ground and, therefore, where rainwater accumulates. It has no drain.

A combined IRT and GPR study was carried out to analyze the effect of moisture on the wall paintings. The IRT method focused on the paintings, while GPR was applied to the floor to investigate the water entry and possible moisture by capillarity.

5.3.1. Methodologies. The GPR survey was conducted using a RAMAC system from MALÅ Geoscience, with a CUII control unit and a 500 MHz antenna. The setting parameters were 3 cm of trace-interval and a total time window of 78 ns composed of 516 samples by trace. The equipment was mounted on a survey cart with an odometer wheel as triggering. The acquisition was based on single antenna 3D GPR methodologies. A grid of parallel profiles spaced 10 cm was collected on the floor at the northern wing (see Figure 10). A total of 19 profile lines were acquired, covering approximately 25 m^2.

The GPR signals received were processed with the ReflexW software, using the following filters: time zero correction, subtract-mean (dewow), gain function, subtracting average, and bandpass (butterworth). The 3D cube and time-slices were elaborated with the same software.

The thermographic camera used was the same as in the previous cases (NEC TH9260). The ambient conditions in the Church (20°C, 70% relative humidity) were considered due to the high humidity, which required the application of the atmospheric correction to the thermal radiation received by the camera. The area inspected was also the North wall, from the interior side. The main drawback of the inspection was the lack of sun and consequently of thermal excitation, which limited the variety of pathologies to be detected to the most severe ones. The application of thermal excitation to the walls is also not possible in order to avoid any damage to the frescoes in the walls.

5.3.2. Results and Findings. Observing the 3D GPR images produced in Figure 10, the presence of water content in the subsoil is associated with a higher intensity (or amplitude) of the radar signal. Figure 10(a) shows the time-slice at 50 cm in depth, in which two reflections were interpreted (highlighted into red boxes) that most likely correspond to the foundation of the attached columns. On the other hand, Figure 10(b) presents the time-slice at a depth of 60 cm, in which two footprints are interpreted

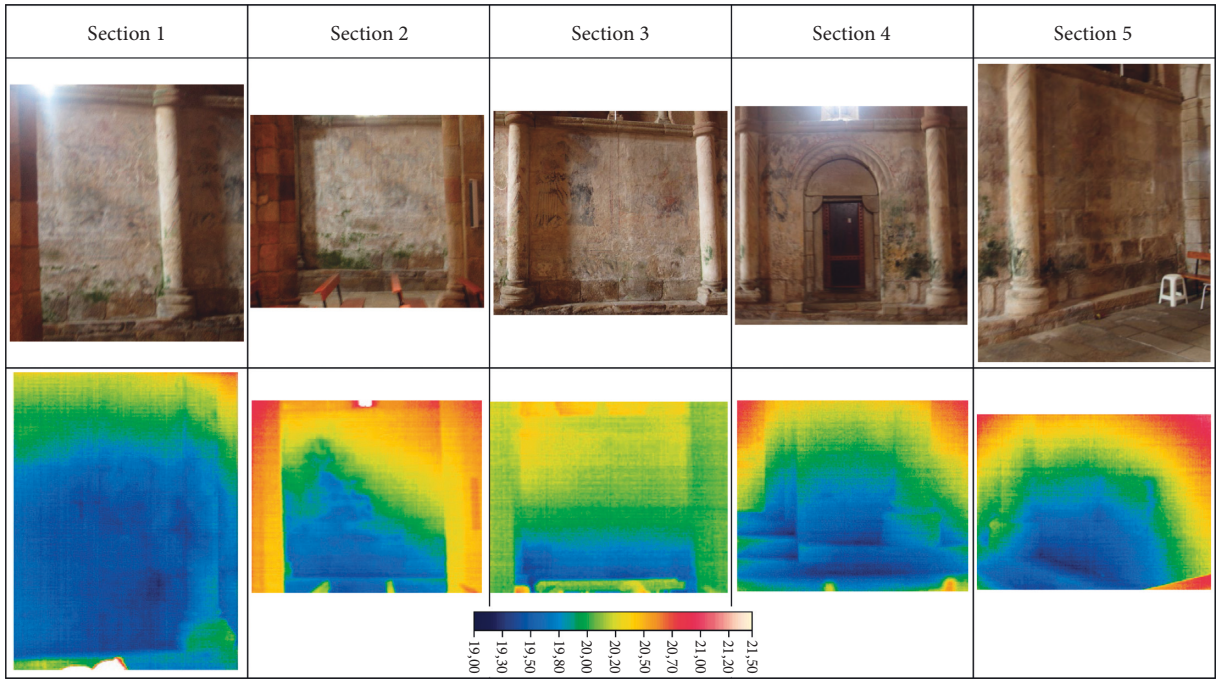

Figure 11: Thermographic inspection of the Moraime church. The color palette applied is the same for all images, showing temperatures between 21.5°C and 18.0°C.

around the columns (red lines) that might be indicating water infiltration.

The thermographic inspection corroborates the detection of moisture as the main pathology in the Church: it appears as a lower temperature area in the images, due to the higher thermal inertia of water (Figure 11). The images of all sections show the presence of moisture in the lower part of the walls, as a sign of water capillary action. This pathology is coherent with the presence of water on the ground detected by the GPR inspection. In Sections 2 and 4, where efflorescence and mold were visible to the eye, the higher effect of the presence of water hid the thermal signs of these pathologies on the thermal images.

In this application, the combination of the GPR and IRT techniques implies the completeness of the study, including both the ground and the walls for a clearer understanding of the situation and for a more integral interpretation of the phenomena occurring in the Church and causing possible damage to the frescoes.

6. Conclusions and Future Perspectives

In this study, an exhaustive review of the state-of-the-art of application of IRT and GPR to building assessment is developed, with special emphasis on applications that integrate both technologies. Specifically, a brief description of each technology and a comparison between their individual and common advantages in the building sector is performed (Section 2). After that, the methodology performed in this review process (Section 3), and the most relevant references, together with the inspection tools used in each case, are detailed by indicating the building materials studied and their specific application according to one of the following three objectives to be achieved: structural safety (Section 4.1), energy efficiency and well-being (Section 4.2), and heritage preservation (Section 4.3). At the end, it is presented three different case studies, with the aim of illustrating the potential of the combined use of IRT and GPR in building assessment from the three objectives defined (Section 5).

After an analysis of the work, the following points can be highlighted as final remarks:

(i) IRT and GPR are capable of detecting the position and mapping the extent of any anomaly, superficial and shallow level with IRT and deeper level with GPR, regardless of the nature of the anomaly. In structural safety, the identification of degradation, cracks, fractures, voids, delamination, detachment, and corrosion is within the reach of both NDTs. The same is true for identifying moisture when assessing building energy efficiency and well-being. Delamination, cracking, cavities and moisture in historic buildings are also covered by IRT and GPR, including small-scale elements such as frescoes, paintings, and marquetry, among others.

(ii) The combination of both inspection tools allows for both a double verification of the findings obtained with each and to complement the information acquired. For instance, in the case of the inspection of an HVAC system, the GPR detects the actual configuration of a radiant floor heating circuit system, while the IRT allows the detection of the pipes in operation. Thus, by combining both techniques, malfunctions can be identified [55].

Another case is moisture analysis, with GPR identifying the origin and source of moisture, and IRT providing information at surface level. Together, they determine the movement of moisture through the wall [18].

(iii) Due to the higher depth range of GPR, it is common to use the latter technique for the detection of hidden targets or structural elements and the estimation of the thickness and quality of walls, although there are some works with IRT for the same task, in case of using active IRT. This preference for the choice of GPR also applies when inspecting internal rebars and monitoring subsidence and settlement phenomenon for the same reason. The opposite would happen for the estimation of the U-value parameter for energy purposes, where the analysis of the surface behavior of the building materials versus the internal behavior prevails, using in this case IRT. The same applies when identifying thermal bridges and air infiltration.

(iv) The common practice of applying several NDTs in addition to IRT and GPR for the same case study, regardless of the building material, objective and application addressed. With this, the verification of the findings is supported, and the results are complemented for a more complete and better-quality building inspection. Laser scanning is a common NDT to use with both GPR and IRT, regardless of its application, given the geometric information provided by this technology. With the integration of laser scanning, 3D GPR and 3D IRT data are obtained. In addition to GPR, ultrasonic and ERT technologies are widely employed for walls and foundation inspections, respectively, in order to complement each other. As for IRT, surface moisture meters and heat flux meters are used for comparison and double checking of results to detect moisture as well as to estimate the U-value, respectively. The blower door test is used to support the detection of air infiltration with IRT. Photogrammetry is an NDT that is also used to generate IRT 3D data.

(v) Studies combining IRT and GPR for building assessment have shown an exponential increase in interest since 2000. Most were published since 2015, with a substantial jump from previous years and with 7–8 publications per year since 2018. Most of the publications reviewed were articles, with 87 publications (87.9%), followed by conference papers and book chapters with 10 (9.9%) and 2 (2.2%) publications, respectively. An equal distribution has been found over the years regarding the number of publications per objective, with 32% in structural safety, with 35% in energy efficiency and user well-being, and with 33% in heritage preservation, respectively.

(vi) The limitations found in this review process were the inaccessibility of some publications because they belong to publishers with no or restricted number of agreements for free access with universities. In addition, some publications were discarded because they were difficult to read, especially due to the lack of a clear description of the case studies analyzed and their purposes.

After the demonstration of the well-defined application of IRT and GPR in the building sector, future lines should be followed in the maturation of the joint application of both technologies. Specifically, they should be jointly directed toward the integration of the results in Building Information Modeling (BIM) and Digital Twins. BIM and Digital Twins are the current protocol being implemented as a communication bridge between inspection tools and users, and directed toward building 4.0. Devices/robots will also play a fundamental role in collecting data in areas that are difficult to access, especially in the case of GPR, and Artificial Intelligence (AI) models to process and interpret the complexity of the IRT and GPR data acquired.

Conflicts of Interest

The authors declare that there are no conflicts of interest regarding the publication of this paper.

Acknowledgments

Iván Garrido acknowledges the Project PDC2021-121239-C32 funded by MCIN/AEI/10.13039/501100011033 and by the European Union Next GenerationEU/PRTR for the given human resources. Mercedes Solla acknowledges the grant RYC2019–026604–I funded by MCIN/AEI/10.13039/501100011033 and by "ESF Investing in your future."

References

[1] F. Hall and R. Greeno, *Building Services Handbook*, Routledge, England, UK, 2017.

[2] H. M. Yilmaz, M. Yakar, S. A. Gulec, and O. N. Dulgerler, "Importance of digital close-range photogrammetry in documentation of cultural heritage," *Journal of Cultural Heritage*, vol. 8, no. 4, pp. 428–433, 2007.

[3] International Organization for Standardization, *ISO and Construction*, International Organization for Standardization, Geneva, Switzerland, 2017.

[4] Y. Fujimoto, "Information standards for cultural heritage with the ISO 191XX series," in *Proceedings of the in 22nd CIPA Symposium*, Kyoto, Japan, October 2009.

[5] I. Flores-Colen and J. De Brito, "A systematic approach for maintenance budgeting of buildings façades based on predictive and preventive strategies," *Construction and Building Materials*, vol. 24, no. 9, pp. 1718–1729, 2010.

[6] Iso, "ISO - ISO/TC 135 - non-destructive testing," 2022, https://www.iso.org/committee/52398.html.

[7] S. Dorafshan and M. Maguire, "Bridge inspection: human performance, unmanned aerial systems and automation," *Journal of Civil Structural Health Monitoring*, vol. 8, no. 3, pp. 443–476, Jul. 2018.

[8] M. Solla and B. Riveiro, *Non-Destructive Techniques for the Evaluation of Structures and Infrastructure*, CRC Press, Boca Raton, FA, USA, 2016.

[9] A. Hussain and S. Akhtar, "Review of non-destructive tests for evaluation of historic masonry and concrete structures," *Arabian Journal for Science and Engineering*, vol. 42, no. 3, pp. 925–940, 2017.

[10] Y. El Masri and T. Rakha, "A scoping review of non-destructive testing (NDT) techniques in building performance diagnostic inspections," *Construction and Building Materials*, vol. 265, Article ID 120542, 2020.

[11] B. Tejedor, E. Lucchi, D. Bienvenido-Huertas, and I. Nardi, "Non-destructive techniques (NDT) for the diagnosis of heritage buildings: traditional procedures and futures perspectives," *Energy and Buildings*, vol. 263, Article ID 112029, 2022.

[12] F. P. Incropera, D. P. DeWitt, T. L. Bergman, and A. S. Lavine, *Fundamentals of Heat and Mass Transfer*, Wiley, Hoboken, NJ, USA, 1996.

[13] M. Vollmer and K.-P. Möllmann, *Infrared thermal Imaging: Fundamentals, Research and Applications*, John Wiley & Sons, Hoboken, NJ, USA, 2017.

[14] I. Garrido, S. Lagüela, R. Otero, and P. Arias, "Thermographic methodologies used in infrastructure inspection: a review—data acquisition procedures," *Infrared Physics & Technology*, vol. 111, Article ID 103481, 2020.

[15] I. Garrido, S. Lagüela, R. Otero, and P. Arias, "Thermographic methodologies used in infrastructure inspection: a review—post-processing procedures," *Applied Energy*, vol. 266, Article ID 114857, 2020.

[16] N. Ida and N. Meyendorf, *Handbook of Advanced Nondestructive Evaluation*, Springer International Publishing, New York, NY, USA, 2019.

[17] A. P. Annan, *GPR Principles, Procedures & Applications; Sensors and Software*, Sensors & Software Incorporated, Mississauga, ON, Canada, 2003.

[18] I. Garrido, M. Solla, S. Lagüela, and N. Fernández, "IRT and GPR techniques for moisture detection and characterisation in buildings," *Sensors*, vol. 20, no. 22, p. 6421, 2020.

[19] I. Petrosyants, "IR thermography system for control and monitoring of energy saving and safety in heating and electrical equipment of housing services," in *Proceedings of the 11th International Conference on Quantitative InfraRed Thermography*, Naples, Italy, June 2012.

[20] X. Núñez-Nieto, M. Solla, A. Novo, and H. Lorenzo, "Three-dimensional ground-penetrating radar methodologies for the characterization and volumetric reconstruction of underground tunneling," *Construction and Building Materials*, vol. 71, pp. 551–560, 2014.

[21] V. Perez-Gracia, O. Caselles, J. Clapes, and S. Santos-Assuncao, "GPR building inspection: examples of building structures assessed with Ground Penetrating Radar," in *Proceedings of the 9th International Workshop on Advanced Ground Penetrating Radar, IWAGPR*, Edinburgh, UK, June 2017.

[22] M. D. Gehrig, D. V Morris, and J. T. Bryant, "Ground Penetrating Radar for Concrete Evaluation Studies," in *Proceedings of the Found. Perform. Assoc. Meet*, Stroudsburg, PA, USA, March 2004.

[23] M. Yumnam, H. Gupta, D. Ghosh, and J. Jaganathan, "Inspection of concrete structures externally reinforced with FRP composites using active infrared thermography: a review," *Construction and Building Materials*, vol. 310, Article ID 125265, 2021.

[24] H. Lorenzo, V. Cuéllar, and M. C. Hernández, "Close range radar remote sensing of concrete degradation in a textile factory floor," *Journal of Applied Geophysics*, vol. 47, no. 3–4, pp. 327–336, Jul. 2001.

[25] E. Bauer, E. Pavón, E. Barreira, and E. Kraus De Castro, "Analysis of building facade defects using infrared thermography: laboratory studies," *Journal of Building Engineering*, vol. 6, pp. 93–104, Jun. 2016.

[26] E. Bauer, P. M. Milhomem, and L. A. G. Aidar, "Evaluating the damage degree of cracking in facades using infrared thermography," *Journal of Civil Structural Health Monitoring*, vol. 8, no. 3, pp. 517–528, Jul. 2018.

[27] D. G. Aggelis, E. Z. Kordatos, D. V. Soulioti, and T. E. Matikas, "Combined use of thermography and ultrasound for the characterization of subsurface cracks in concrete," *Construction and Building Materials*, vol. 24, no. 10, pp. 1888–1897, 2010.

[28] G. De Donno, L. Di Giambattista, and L. Orlando, "High-resolution investigation of masonry samples through GPR and electrical resistivity tomography," *Construction and Building Materials*, vol. 154, pp. 1234–1249, 2017.

[29] S. Negri and M. A. Aiello, "High-resolution GPR survey for masonry wall diagnostics," *Journal of Building Engineering*, vol. 33, Article ID 101817, 2021.

[30] G. Leucci, S. Negri, and M. T. Carrozzo, "Ground Penetrating Radar (GPR): an application for evaluating the state of maintenance of the building coating," *Annals of Geophysics*, vol. 46, no. 3, 2003.

[31] V. Pérez-Gracia, F. G. García García, and I. Rodriguez Abad, "GPR evaluation of the damage found in the reinforced concrete base of a block of flats: a case study," *NDT & E International*, vol. 41, no. 5, pp. 341–353, Jul. 2008.

[32] M. Bavusi, A. Loperte, V. Lapenna, and F. Soldovieri, "Rebars and defects detection by a GPR survey at a L'Aquila school damaged by the earthquake of April 2009," in *Proceedings of the 13th International Conference on Ground Penetrating Radar*, Lecce, Italy, 2010.

[33] A. Villarino, B. Riveiro, D. Gonzalez-Aguilera, and L. J. Sánchez-Aparicio, "The integration of geotechnologies in the evaluation of a wine cellar structure through the finite element method," *Remote Sensing*, vol. 6, no. 11, pp. 11107–11126, 2014.

[34] P. Cotič, Z. Jagličić, V. Bosiljkov, and E. Niederleithinger, "GPR and IRT thermography for near-surface defect detection in building structures," in *Proceedings of the XII International Conference of the Slovenian Society for Non-Destrutive Testing*, Göteborg, Sweden, June 2013.

[35] P. Cotič, D. Kolarič, V. B. Bosiljkov, V. Bosiljkov, and Z. Jagličić, "Determination of the applicability and limits of void and delamination detection in concrete structures using infrared thermography," *NDT & E International*, vol. 74, pp. 87–93, Sep. 2015.

[36] T. Lourenço, L. Matias, and P. Faria, "Anomalies detection in adhesive wall tiling systems by infrared thermography," *Construction and Building Materials*, vol. 148, pp. 419–428, Sep. 2017.

[37] I. Garrido, E. Barreira, R. Msf Almeida, and S. Lagüela, "Introduction of active thermography and automatic defect segmentation in the thermographic inspection of specimens of ceramic tiling for building façades," *Infrared Physics & Technology*, vol. 121, Article ID 104012, 2022.

[38] E. Barreira, S. S. de Freitas, V. P. de Freitas, and J. M. P. Q. Delgado, "Infrared thermography application in

buildings diagnosis: a proposal for test procedures," *Adv. Struct. Mater.*vol. 36, pp. 91–117, 2013.

[39] S. A. Keo, F. Brachelet, F. Breaban, and D. Defer, "Steel detection in reinforced concrete wall by microwave infrared thermography," *NDT & E International*, vol. 62, pp. 172–177, Mar. 2014.

[40] B. Szymanik, P. K. Frankowski, T. Chady, and C. John Chelliah, "Detection and inspection of steel bars in reinforced concrete structures using active infrared thermography with microwave excitation and eddy current sensors," *Sensors*, vol. 16, no. 2, p. 234, 2016.

[41] F. Zhou, Z. Chen, H. Liu, J. Cui, B. F. Spencer, and G. Fang, "Simultaneous estimation of rebar diameter and cover thickness by a GPR-EMI dual sensor," *Sensors*, vol. 18, no. 9, p. 2969.

[42] Z. Xiang, A. Rashidi, and G. Ou, "An improved convolutional neural network system for automatically detecting rebar in GPR data, " comput. Civ. Eng. 2019 data, sensing, anal. - sel. Pap. From," *ASCE Int. Conf. Comput. Civ. Eng.*, pp. 422–429, 2019.

[43] H. Liu, C. Lin, J. Cui, L. Fan, X. Xie, and B. F. Spencer, "Detection and localization of rebar in concrete by deep learning using ground penetrating radar," *Automation in Construction*, vol. 118, Article ID 103279, 2020.

[44] Z. Xiang, G. Ou, and A. Rashidi, "Robust cascaded frequency filters to recognize rebar in GPR data with complex signal interference," *Automation in Construction*, vol. 124, Article ID 103593, 2021.

[45] D. De Domenico, D. Campo, and A. Teramo, "FDTD modelling in high-resolution 2D and 3D GPR surveys on a reinforced concrete column in a double wall of hollow bricks," *Near Surface Geophysics*, vol. 11, no. 1, pp. 29–40, 2013.

[46] M. Solla, S. Lagüela, N. Fernández, and I. Garrido, "Assessing rebar corrosion through the combination of nondestructive GPR and IRT methodologies," *Remote Sensing*, vol. 11, no. 14, p. 1705, 2019.

[47] S. Baek, W. Xue, M. Q. Feng, and S. Kwon, "Nondestructive corrosion detection in RC through integrated heat induction and IR thermography," *Journal of Nondestructive Evaluation*, vol. 31, no. 2, pp. 181–190, 2012.

[48] S. Na and I. Paik, "Application of thermal image data to detect rebar corrosion in concrete structures," *Applied Sciences*, vol. 9, no. 21, p. 4700.

[49] B. Goffin, N. Banthia, and N. Yonemitsu, "Use of infrared thermal imaging to detect corrosion of epoxy coated and uncoated rebar in concrete," *Construction and Building Materials*, vol. 263, Article ID 120162, 2020.

[50] E. Taştan, S. Koşaroğlu, and F. Bilim, "Identifying of structural elements of building using Ground penetrating radar (GPR): a case study of the Cumhuriyet University, Turkey," *Bitlis Eren University Journal of Science and Technology*, vol. 7, no. 1, pp. 22–26, 2017.

[51] K. Dinh, T. Zayed, and A. Tarussov, "GPR image analysis for corrosion mapping in concrete slabs," in *Proceedings of the CSCE 2013 General Conference*, Montreal, Canada, June 2013.

[52] L. Capozzoli, G. De Martino, M. Polemio, and E. Rizzo, "Geophysical techniques for monitoring settlement phenomena occurring in reinforced concrete buildings," *Surveys in Geophysics*, vol. 41, no. 3, pp. 575–604, May 2020.

[53] M. Solla and N. Fernández, "GPR analysis to detect subsidence: a case study on a loaded reinforced concrete pavement," *International Journal of Pavement Engineering*, 2022.

[54] P. Jena and R. Gupta, "Estimation of delamination thickness in a multi-layered thermally thin structure by step heating thermography," *Composite Structures*, vol. 281, Article ID 114988, 2022.

[55] S. Lagüela-López, M. Solla-Carracelas, L. Díaz-Vilariño, and J. Armesto-González, "Inspection of radiant heating floor applying non-destructive testing techniques: GPR and IRT," *Dyna*, vol. 82, no. 190, pp. 221–226, 2015.

[56] I. Garrido, S. Lagüela, S. Sfarra, F. J. Madruga, and P. Arias, "Automatic detection of moistures in different construction materials from thermographic images," *Journal of Thermal Analysis and Calorimetry*, vol. 138, no. 2, pp. 1649–1668, 2019.

[57] E. Edis, I. Flores-Colen, and J. de Brito, "Quasi-quantitative infrared thermographic detection of moisture variation in facades with adhered ceramic cladding using principal component analysis," *Building and Environment*, P1, vol. 94, , pp. 97–108, 2015.

[58] I. Garrido, S. Lagüela, Q. Fang, and P. Arias, "Introduction of the combination of thermal fundamentals and Deep Learning for the automatic thermographic inspection of thermal bridges and water-related problems in infrastructures," *Quantitative InfraRed Thermography Journal*, pp. 1–25, 2022.

[59] R. Agliata, T. A. Bogaard, R. Greco, L. Mollo, E. C. Slob, and S. C. Steele-Dunne, "Non-invasive estimation of moisture content in tuff bricks by GPR," *Construction and Building Materials*, vol. 160, pp. 698–706, Jan. 2018.

[60] I. Garrido, S. Lagüela, P. Arias, and J. Balado, "Thermal-based analysis for the automatic detection and characterization of thermal bridges in buildings," *Energy and Buildings*, vol. 158, pp. 1358–1367, 2018.

[61] M. O'Grady, A. A. Lechowska, and A. M. Harte, "Infrared thermography technique as an in-situ method of assessing heat loss through thermal bridging," *Energy and Buildings*, vol. 135, pp. 20–32, Jan. 2017.

[62] M. O'Grady, A. A. Lechowska, and A. M. Harte, "Quantification of heat losses through building envelope thermal bridges influenced by wind velocity using the outdoor infrared thermography technique," *Applied Energy*, vol. 208, pp. 1038–1052, 2017.

[63] G. Baldinelli, F. Bianchi, A. Rotili et al., "A model for the improvement of thermal bridges quantitative assessment by infrared thermography," *Applied Energy*, vol. 211, pp. 854–864, Feb. 2018.

[64] S. Sfarra, A. Cicone, B. Yousefi, C. Ibarra-Castanedo, S. Perilli, and X. Maldague, "Improving the detection of thermal bridges in buildings via on-site infrared thermography: the potentialities of innovative mathematical tools," *Energy and Buildings*, vol. 182, pp. 159–171, Jan. 2019.

[65] C. Kim, J. S. Choi, H. Jang, and E. J. Kim, "Automatic detection of linear thermal bridges from infrared thermal images using neural network," *Applied Sciences*, vol. 11, no. 3, p. 931, 2021.

[66] D. Antón and J.-L. Amaro-Mellado, "Engineering graphics for thermal assessment: 3D thermal data visualisation based on infrared thermography, GIS and 3D point cloud processing software," *Symmetry*, vol. 13, no. 2, p. 335, Feb. 2021.

[67] B. Tejedor, M. Casals, M. Gangolells, and X. Roca, "Quantitative internal infrared thermography for determining in-situ thermal behaviour of façades," *Energy and Buildings*, vol. 151, pp. 187–197, Sep. 2017.

[68] I. Danielski and M. Fröling, "In situ measurements of thermal properties of building fabrics using thermography

under non-steady state heat flow conditions," *Infrastructure*, vol. 3, no. 3, p. 20, 2018.

[69] R. Albatici, A. M. Tonelli, and M. Chiogna, "A comprehensive experimental approach for the validation of quantitative infrared thermography in the evaluation of building thermal transmittance," *Applied Energy*, vol. 141, pp. 218–228, Mar. 2015.

[70] D. Patel, J. E. Schmiedt, M. Röger, and B. Hoffschmidt, "Approach for external measurements of the heat transfer coefficient (U-value) of building envelope components using UAV based infrared thermography," in *Proceedings of the 14th Quantitative InfraRed Thermography Conference*, pp. 379–386, Berlin, Germany, June 2018.

[71] M. Mahmoodzadeh, V. Gretka, K. Hay, C. Steele, and P. Mukhopadhyaya, "Determining overall heat transfer coefficient (U-Value) of wood-framed wall assemblies in Canada using external infrared thermography," *Building and Environment*, vol. 199, Article ID 107897, 2021.

[72] B. Tejedor, E. Barreira, R. M. S. F. Almeida, and M. Casals, "Thermographic 2D U-value map for quantifying thermal bridges in building façades," *Energy and Buildings*, vol. 224, Article ID 110176, 2020.

[73] S. Lagüela, L. Díaz-Vilariño, J. Armesto, and P. Arias, "Non-destructive approach for the generation and thermal characterization of an as-built BIM," *Construction and Building Materials*, vol. 51, pp. 55–61, Jan. 2014.

[74] D. González-Aguilera, P. Rodriguez-Gonzalvez, J. Armesto, and S. Lagüela, "Novel approach to 3D thermography and energy efficiency evaluation," *Energy and Buildings*, vol. 54, pp. 436–443, Nov. 2012.

[75] W. Natephra, A. Motamedi, N. Yabuki, and T. Fukuda, "Integrating 4D thermal information with BIM for building envelope thermal performance analysis and thermal comfort evaluation in naturally ventilated environments," *Building and Environment*, vol. 124, pp. 194–208, Nov. 2017.

[76] C. Lerma, E. Barreira, and R. M. S. F. Almeida, "A discussion concerning active infrared thermography in the evaluation of buildings air infiltration," *Energy and Buildings*, vol. 168, pp. 56–66, Jun. 2018.

[77] E. Barreira, R. M. S. F. Almeida, and M. Moreira, "An infrared thermography passive approach to assess the effect of leakage points in buildings," *Energy and Buildings*, vol. 140, pp. 224–235, Apr. 2017.

[78] W. Liu, X. Zhao, and Q. Chen, "A novel method for measuring air infiltration rate in buildings," *Energy and Buildings*, vol. 168, pp. 309–318, Jun. 2018.

[79] T. Kalamees, Ü. Alev, and M. Pärnalaas, "Air leakage levels in timber frame building envelope joints," *Building and Environment*, vol. 116, pp. 121–129, May 2017.

[80] R. Gil-Valverde, D. Tamayo-Alonso, A. Royuela-del-Val, I. Poza-Casado, A. Meiss, and M. Á. Padilla-Marcos, "Three-dimensional characterization of air infiltration using infrared thermography," *Energy and Buildings*, vol. 233, 2021.

[81] A. Royuela-del-Val, M. Á. Padilla-Marcos, A. Meiss, P. Casaseca-de-la-Higuera, and J. Feijó-Muñoz, "Air infiltration monitoring using thermography and neural networks," *Energy and Buildings*, vol. 191, pp. 187–199, May 2019.

[82] M. Solla, L. M. S. Goncalves, G. Goncalves et al., "A building information modeling approach to integrate geomatic data for the documentation and preservation of cultural heritage," *Remote Sensing*, vol. 12, no. 24, p. 4028, 2020.

[83] G. Diana and S. Fais, "IR thermography and ultrasonic investigations in the cultural heritage field," in *Proceedings of the 15th International Conference on "Cultural Heritage and New Technologies*, pp. 643–648, Nicosia, Cyprus, June 2010.

[84] C. Ç. Yalçıner, A. Büyüksaraç, and Y. C. Kurban, "Non-destructive damage analysis in Kariye (Chora) Museum as a cultural heritage building," *Journal of Applied Geophysics*, vol. 171, Article ID 103874, 2019.

[85] V. Pérez-Gracia, J. O. Caselles, J. Clapés, G. Martinez, and R. Osorio, "Non-destructive analysis in cultural heritage buildings: evaluating the Mallorca cathedral supporting structures," *NDT & E International*, vol. 59, pp. 40–47, Oct. 2013.

[86] M. Rasol, V. Perez-Gracia, F. M. Fernandes, J. C. Pais, S. Santos-Assunçao, and J. S. Roberts, "Ground penetrating radar system: principles," in *Handbook of Cultural Heritage Analysis*, S. D'Amico and V. Venuti, Eds., pp. 705–738, Springer International Publishing, New York, NY, USA, 2022.

[87] D. C. B. Cintra, P. M. B. Manhães, F. M. C. P. Fernandes, D. M. Roehl, J. T. Araruna Júnior, and E. S. Sánchez Filho, "Evaluation of the GPR (1.2 GHz) technique in the characterization of masonry shells of the Theatro Municipal do Rio de Janeiro," *Revista IBRACON de Estruturas e Materiais*, vol. 13, no. 2, pp. 274–297, Jun. 2020.

[88] H. Glavaš, M. Hadzima-Nyarko, I. Haničar Buljan, and T. Barić, "Locating hidden elements in walls of cultural heritage buildings by using infrared thermography," *Buildings*, vol. 9, no. 2, p. 32, 2019.

[89] S. Sfarra, E. Marcucci, D. Ambrosini, and D. Paoletti, "Infrared exploration of the architectural heritage: from passive infrared thermography to hybrid infrared thermography (HIRT) approach," *Materiales de Construcción*, vol. 66, no. 323, p. e094, 2016.

[90] C. Ibarra-Castanedo, S. Sfarra, M. Klein, and X. Maldague, "Solar loading thermography: time-lapsed thermographic survey and advanced thermographic signal processing for the inspection of civil engineering and cultural heritage structures," *Infrared Physics & Technology*, vol. 82, pp. 56–74, May 2017.

[91] S. Santos-Assunçao, K. Dimitriadis, Y. Konstantakis, V. Perez-Gracia, E. Anagnostopoulou, and R. Gonzalez-Drigo, "Ground-penetrating radar evaluation of the ancient Mycenaean monument Tholos Acharnon tomb," *Near Surface Geophysics*, vol. 13, pp. 197–205, 2015.

[92] R. W. Arndt, "Square pulse thermography in frequency domain as adaptation of pulsed phase thermography for qualitative and quantitative applications in cultural heritage and civil engineering," *Infrared Physics & Technology*, vol. 53, no. 4, pp. 246–253, Jul. 2010.

[93] G. M. Carlomagno, R. Di Maio, C. Meola, and N. Roberti, "Infrared thermography and geophysical techniques in cultural heritage conservation," *Quantitative InfraRed Thermography Journal*, vol. 2, no. 1, pp. 5–24, 2005.

[94] B. Johnston, A. Ruffell, J. McKinley, and P. Warke, "Detecting voids within a historical building façade: a comparative study of three high frequency GPR antenna," *Journal of Cultural Heritage*, vol. 32, pp. 117–123, Jul. 2018.

[95] M. Guadagnuolo, G. Faella, A. Donadio, and L. Ferri, "Integrated evaluation of the church of S. Nicola di Mira: conservation versus safety," *NDT & E International*, vol. 68, pp. 53–65, Dec. 2014.

[96] N. Işık, F. M. Halifeoğlu, and S. İpek, "Detecting the ground-dependent structural damages in a historic mosque by employing GPR," *Journal of Applied Geophysics*, vol. 199, Article ID 104606, 2022.

[97] I. Catapano, G. Ludeno, F. Soldovieri, F. Tosti, and G. Padeletti, "Structural assessment via ground penetrating radar at the consoli palace of gubbio (Italy)," *Remote Sensing*, vol. 10, no. 2, p. 45, 2017.

[98] M. I. Martínez-Garrido, R. Fort, M. Gómez-Heras, J. Valles-Iriso, and M. J. Varas-Muriel, "A comprehensive study for moisture control in cultural heritage using non-destructive techniques," *Journal of Applied Geophysics*, vol. 155, pp. 36–52, Aug. 2018.

[99] E. Diz-Mellado, "Non-destructive testing and Finite Element Method integrated procedure for heritage diagnosis: the Seville Cathedral case study," *Journal of Building Engineering*, vol. 37, Article ID 102134, 2021.

[100] I. Garrido, S. Lagüela, S. Sfarra, and M. Solla, "ALGORITHMS for the AUTOMATIC DETECTION and CHARACTERIZATION of PATHOLOGIES in HERITAGE ELEMENTS from THERMOGRAPHIC IMAGES," *Remote Sensing and Spatial Information Sciences - ISPRS Archives*, vol. 42, 2019.

[101] R. Cataldo, A. De Donno, G. De Nunzio, G. Leucci, L. Nuzzo, and S. Siviero, "Integrated methods for analysis of deterioration of cultural heritage: the Crypt of Cattedrale di Otranto," *Journal of Cultural Heritage*, vol. 6, no. 1, pp. 29–38, Jan. 2005.

[102] I. Nardi, S. Sfarra, D. Ambrosini, and D. Dominici, "Complementarity of terrestrial laser scanning and IR thermography for the diagnosis of cultural heritage: the case of Pacentro Castle," in *Proceedings of the 13th International Workshop on Advanced Infrared Technology & Applications*, pp. 263–266, Florence, Italy, September 2015.

[103] M. Danese, M. Sileo, and N. Masini, "Geophysical methods and spatial information for the analysis of decaying frescoes," *Surveys in Geophysics*, vol. 39, no. 6, pp. 1149–1166, Nov, 2018.

[104] G. Cadelano, P. Bison, A. Bortolin et al., "Monitoring of historical frescoes by timed infrared imaging analysis," *Opto-Electronics Review*, vol. 23, no. 1, pp. 102–108, Jan. 2015.

[105] K. Mouhoubi, J. L. Bodnar, J.-M. Vallet, and V. Detalle, "Stimulated infrared thermography application to the conservation of heritage wall paintings: interest of a material and software combined approach," *Optics for Arts, Architecture, and Archaeology VII*, vol. 11058, pp. 39–44, Article ID 110580H, 2019.

[106] I. Garrido, S. Lagüela, S. Sfarra, and P. Arias, "Development of thermal principles for the automation of the thermographic monitoring of cultural heritage," *Sensors*, vol. 20, no. 12, p. 3392, 2020.

[107] A. O. Chulkov, S. Sfarra, N. Saeed et al., "Evaluating quality of marquetries by applying active IR thermography and advanced signal processing," *Journal of Thermal Analysis and Calorimetry*, vol. 143, no. 5, pp. 3835–3848, 2021.

[108] I. Garrido, J. Erazo-Aux, S. Laguela et al., "Introduction of deep learning in thermographic monitoring of cultural heritage and improvement by automatic thermogram pre-processing algorithms," *Sensors*, vol. 21, no. 3, p. 750, 2021.

[109] A. Calia, M. Lettieri, G. Leucci, L. Matera, R. Persico, and M. Sileo, "The mosaic of the crypt of St. Nicholas in Bari (Italy): integrated GPR and laboratory diagnostic study," *Journal of Archaeological Science*, vol. 40, no. 12, pp. 4162–4169, 2013.

[110] I. Campione, F. Lucchi, N. Santopuoli, and L. Seccia, "3D thermal imaging system with decoupled acquisition for industrial and cultural heritage applications," *Applied Sciences*, vol. 10, no. 3, p. 828, 2020.

[111] L. Evangelista, F. de Silva, A. d'Onofrio et al., "Application of ERT and GPR geophysical testing to the subsoil characterization of cultural heritage sites in Napoli (Italy)," *Measurement*, vol. 104, pp. 326–335, Jul. 2017.

[112] M. Dabas, C. Camerlynck, and P. F. I. Camps, "Simultaneous use of electrostatic quadrupole and GPR in urban context: investigation of the basement of the Cathedral of Girona (Catalunya, Spain)," *Geophysics*, vol. 65, no. 2, pp. 526–532, 2000.

[113] M. Rucka, E. Wojtczak, and M. Zielińska, "Interpolation methods in GPR tomographic imaging of linear and volume anomalies for cultural heritage diagnostics," *Measurement*, vol. 154, Article ID 107494, 2020.

[114] I. Martínez and E. Martínez, "Qualitative timber structure assessment with passive IR thermography. Case study of sources of common errors," *Case Studies in Construction Materials*, vol. 16, Article ID e00789, 2022.

[115] S. Fontul, M. Solla, H. Cruz, J. S. Machado, and L. Pajewski, "Ground penetrating radar investigations in the noble Hall of são carlos theater in lisbon, Portugal," *Surveys in Geophysics*, vol. 39, no. 6, pp. 1125–1147, 2018.

[116] L. Balík, L. Kudrnáčová, Z. Pavlík, and R. Černý, "Application of infrared thermography in complex moisture inspection of the Schebek Palace," *AIP Conference Proceedings*, vol. 1866, Article ID 040002, 2017.

[117] R. González-Drigo, V. Pérez-Gracia, D. Di Capua, and L. G. Pujades, "GPR survey applied to Modernista buildings in Barcelona: the cultural heritage of the College of Industrial Engineering," *Journal of Cultural Heritage*, vol. 9, no. 2, pp. 196–202, Apr. 2008.